International Journal of Applied Engineering Research ISSN 0973-4562 Volume 10, Number 16 (2015) pp 37030-37037
 https://dx.doi.org/10.37622/IJAER/10.16.2015.37030-37037

Enhanced Mechanical Properties of Tellurium Nanowires Reinforced Epoxy Polymer

Praveen Kumar Balguri
Assistant Professor, School of Aeronautical Sciences, Hindustan University
Chennai – 603103, INDIA

Udayabhaskararao Thumu
Department of Organic Chemistry, Weizmann Institute of science
Rehovot –76100, ISRAEL

D. G. Harris Samuel
Professor, Department of Mechanical Engineering,
Hindustan University, Chennai – 603103, INDIA

Abstract
One dimensional (1D) tellurium nanowires (Te NWs) reinforced epoxy composites have been prepared and the mechanical properties of Te NWs/epoxy nanocomposites with respect to tensile and impact properties were studied. The length and width of the Te NWs used to make Te NWs/epoxy nanocomposites are 697±87 nm and 21±2.5 nm, respectively. Mechanical stirrer dispersion process was used to minimize the agglomeration of Te NWs within the epoxy resin. Plain and Te NWs/epoxy nanocomposites were characterized by X-ray diffraction (XRD) and differential scanning calorimetry (DSC). Remarkable enhancement in the tensile and impact strengths of Te NWs/epoxy nanocomposites is observed in comparison to plain epoxy composite. The impact and tensile strengths were increased by 100 % and 10.6 % with the addition of very little Te NWs content (0.05 Wt. %). The microstructure study of specimens and corresponding fracture surfaces were examined by scanning electron microscopy (SEM). From SEM analysis, we observed the formation of end-to-end and side-to-side assembly of Te NWs into large chain-like arrangements.

Keywords: Te nanowires, Self-assembly, Tensile strength, Impact strength, Mechanical properties, Epoxy resin.

Introduction
Over the past few years, nanomaterials have attracted considerable attention because of their enhanced mechanical,[1-5] electrical,[6,7] magnetic,[7,8] optical[9,10] and chemical properties.[11,12] These novel properties of nanomaterials in comparison to their bulk materials are due to their large surface area to volume ratio and quantum size effects. Nano-forms with different size and shape of the same element can typically exhibit quite different mechanical, optical, electrical and magnetic properties.[13,14] For example, the mechanical properties of spheres and whiskers are different, even though the base element is alumina.[13] The intrinsic mechanical properties are highly influenced by lattice vibration modes of nanoparticles which depend on its shape and symmetry. The changes in lattice vibration modes can occur by changes in the internal structure or in the overall physical dimensions of a nanoparticle. Size and shape related effects influence the internal length scales and resulting properties are often useful for industrial applications.

Mixing of one or more kinds of these potential candidates to the polymers results in new kind of materials called nanocomposites. From the intense scientific study in the area of nanocomposites, it is already proved that the homogeneous reinforcement of 1D or 2D nanomaterials in the host polymer matrix can substantially improve the conductivity, toughness, elasticity, and strength of the polymer material.[15-18] Nanomaterials are also acting as high potential filler materials by creating good interfacial bonding between nanoparticle-polymer interface which is an essential requirement to enhance the mechanical and thermal properties of polymer composites. Enhanced properties of these nanomaterials reinforced composite materials are widely used in defence,[18,19] automobile and aero applications.[20]

In comparison to the bulk materials, additional advantages upon the usage of nanomaterials are 1) reduction in the weight of total nanocomposite 2) greater improvement of the mechanical properties and 3) improved functionality. Nanotechnology has produced various kinds of nanomaterials, which exhibit their unique properties in different fields. Among the choices of host polymer matrix, in particular, epoxy resins are universally used because of their property of irreversible cure, often with strong mechanical properties as well as better temperature and chemical resistance.[21] The possibility of electron beam curing on cationic epoxy resin could also meet the demanding requirements of high-performance composite structures.[21] Epoxy composites are also known to exhibit high tensile strength, Young's modulus, good electrical and thermal insulating properties. These properties of epoxy can be

further improved by the introduction of inorganic fillers, called epoxy nanocomposites. Optical, electrical, magnetic and anticorrosive properties of the epoxy get improved because of the inorganic fillers.[20]

Several nanomaterials such as carbon nanotubes, silver nanoparticles, TiO_2 nanoparticles, Fe_2O_3 nanoparticles etc. have been used as fillers and reports have shown that these nanocomposites are better materials than the conventional epoxy composites. For example, thermal and electrical conductivity of the epoxy composites can be improved by the use of silver[22] and copper nanoparticles as fillers.[23] Magnetism can be successfully imputed by the use of magnetic nanoparticles as fillers.[24] Semiconducting properties and the subsequent applications in the area of photovoltaics can be imputed by the insertion of TiO_2 nanoparticles[25] as well as TiO_2 nanotubes and quantum dots.[26] Carbon nanotube based epoxy composites are useful in various applications because of their light weight and high strength.[16,27,28]

In this study, we specially discuss about the semiconductor nanowires reinforced epoxy composites. In particular, Te NWs are considered as nanofillers for the following reasons: Te is well-known p-type narrow band-gap semiconductor with a direct band gap of 0.35 eV at room temperature. This unique electronic structure of single crystal Te NWs offers potential candidate for photoconductivity, nonlinear optical response, high thermoelectric performance and piezoelectric responsive materials. Te NWs and their derivatives were also suggested as platforms for gas sensing probes, optoelectronic devices, photonic crystals, field-effect devices, self-developing holographic recording devices, radiative cooling devices, and topological insulators, sensors, and magnetic memories.[29-30] In view of the importance of this material, here, we focus on the reinforcement effect of Te NWs on the mechanical strength of epoxy composites. Improvement in the impact and tensile strength can be helpful in fabrication of novel epoxy-based electronic or electromechanical devices.

Here, we report the synthesis, characterization and mechanical property studies of Te NWs reinforced epoxy composites. Unlike gold/silver anisotropic nanomaterials, the synthesis of 1D Te NWs is simpler, highly reproducible and possible to get them in gram scale. The 1D growth of Te seed is due to its unique crystal structure i.e. polymeric structure, consisting of zig-zag hexagonal lattice chains of covalently bound Te atoms in trigonal Tellurium (t-Te). The distance between each adjacent chain is more than covalent bond and less than van der Waals interaction. Overlapping between the antibonding orbitals and the lone-pair orbitals on adjacent chains induces the interchain interactions. This unique structure of Te helps to grow anisotropic one-dimensional structure.[31,32] Several methods such as thermal deposition,[33] hydrothermal,[34] microwave-assisted,[35] and biomolecule-assisted[36] and chemical vapor deposition[37] have been reported for the synthesis of Te NWs. Most of them were done at very high temperatures. For simple, monodisperse and high-yield synthesis of Te NWs, we used a room-temperature protocol reported by Lin *et al.*[31]

.

2. Experimental section

2.1. *Materials*

The matrix material used is epoxy system (Araldite LY 556) and the curing agent is Aradur HY 951 by Huntsman, India. Lab-made Te NWs were used as reinforcement in the epoxy system. All the chemicals used for the synthesis of Te NWs were commercially available and were used without further purification. Sodium Dodecyl Sulfate (SDS, $C_{12}H_{25}O_4SNa$, 99%) was obtained from Acros. Tellurium dioxide (TeO_2, 99.9%) powder by Alfa Aesar. Hydrazine monohydrate ($N_2H_4.H_2O$, 99-100%) by SD Fine Chemicals, India. Deionized water was used throughout the experiment. All glasswares were thoroughly cleansed with aqua regia (3:1 vol% of HCl:HNO_3), rinsed with plenty of deionized water, and then dried in oven at 120 °C prior to use.

2.2. *Instrumentation*

UV-vis spectra were measured with a PerkinElmer Lambda 25 instrument in the range of 200-1100 nm. Transmission electron microscopy (TEM) of Te NWs was carried out with a JEOL 3010, a 300 kV instrument. The samples were drop cast on carbon-coated copper grids and allowed to dry under ambient conditions. Scanning electron microscopic (SEM) analyses was done in a FEI QUANTA- 200 SEM. For SEM measurements, piece of epoxy and Te NWs/epoxy samples were loaded on an indium tin oxide coated conducting glass. Powder XRD patterns of the samples were recorded using a PANalyticalX'pertPro diffractometer. The broken pieces as well as the powder samples of plain and Te NWs/epoxy were subjected to X-ray diffractogram and were collected from 5 to 100 degrees in 2 theta using Cu Ka radiation. DSC was carried out using a NETZSCH DSC 204 instrument under nitrogen atmosphere, at a heating rate of 10 °C/ min.

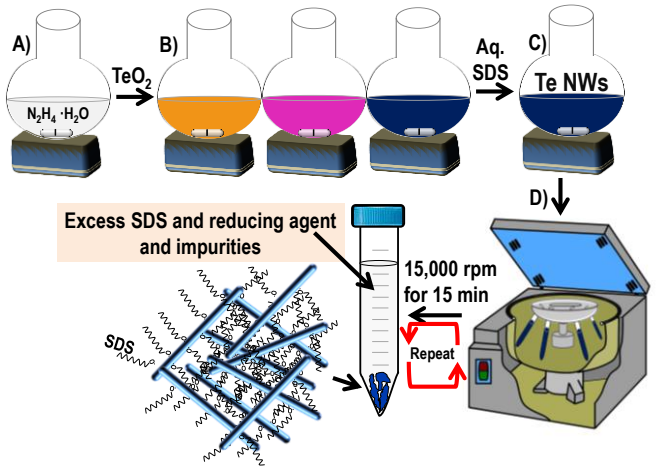

Scheme 1. A) Colorless hydrazine solution ($N_2H_4.H_2O$) acts as reducing agent. B) Slow addition of TeO_2 powder to the solution. Subsequent color changes from colorless to pale yellow, purple and blue color within an hour. Blue color indicates the formation of Te NWs. C) Growth of the Te NWs was arrested by the addition of SDS surfactant. D) Te NWs solution was centrifuged repeatedly. Supernatant contains the excess SDS, reducing agent. The precipitate was Te NWs.

2.3. *Synthesis of Te NWs*

The total synthesis process is given in Scheme 1. Te NWs were prepared by the chemical method introduced by Lin *et al.*[31] In the reaction, 16 mg of TeO_2 powder was slowly added to a round bottom flask containing 10 mL of hydrazine hydrate. The reaction was continuously stirred at room

temperature. The TeO_2 powder was completely dissolved, and the color of the solution changed from colorless to pale yellow, purple and to blue about an hour. The blue color indicates the formation of Te NWs. Then the solution was diluted with 10-fold SDS solution (10 mM), to control the length of the NWs. SDS is organosulfate consisting of a 12-carbon tail attached to a sulfate group. The as-prepared solution was purified by centrifugation at 15,000 rpm for 15 minutes to remove excess hydrazine and SDS. The residue was redispersed in deionized water and centrifuged twice to remove unreacted species and excess and loosely bound SDS. Removal of excess surfactant is important to improve the mechanical properties of the Te NWs/epoxy nanocomposites.

2.4. *Preparation of Specimens*

The fabrication of the composites was carried out through hand lay-up technique. The mould used to prepare epoxy nanocomposites is consists of two soft rectangular aluminum alloy sheets and a single rubber spacer arranged in between as shown in Fig. 1.

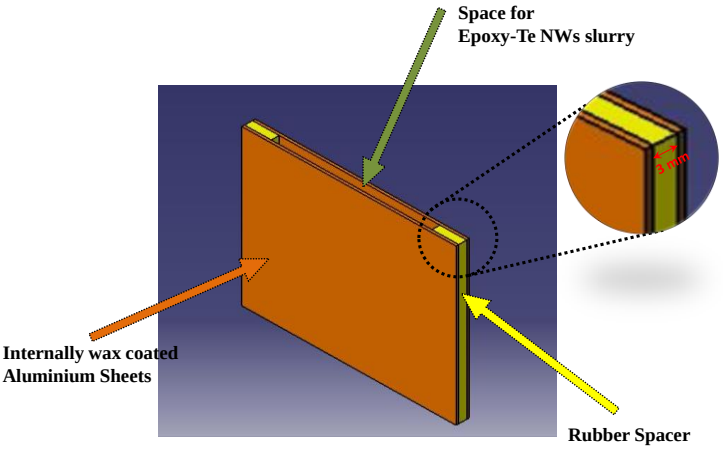

Fig. 1. Schematic representation of the mold used to prepare epoxy nanocomposites.

The thickness of the epoxy specimens is controlled by the thickness of the rubber pacer which is 3 mm. The inner surfaces of aluminum plates were polished to achieve smooth sample surface and every time coated with a very thin layer of wax as a releasing agent.

Epoxy resin and hardener mixture was at ratio of 1: 0.1 by weight. Specimens with loading concentration of 0.05% Te NWs by weight (in solid form) were prepared. The sample was subjected to gentle mechanical stirring in a beaker at ambient conditions for overnight. This long stirring process can help to produce uniform Te NWs/epoxy slurry and allow the epoxy to chemisorb on Te NWs surface for better interface. It is known that epoxy possess many hydroxyl (-OH) groups, have much chemical affinity toward metallic surface of active Te NW surface. Hence -OH groups get attached to the bare surface of Te NWs and helps to create good interfacial bonding between Te NW and epoxy. These nanowires can be visualized as small iron rods in concrete, so it is expected to improve the strength. During the stirring, the color of epoxy changes from colorless to pale blue color indicates uniform mixing of Te NWs with epoxy resin. By placing the mixture in the vacuum for 20 minutes, the gas bubbles generated during the mixing process were removed. Then, the hardener was added and the mixture is stirred well with glass stirring rod. The resulting epoxy mixture was poured into the mould (Fig. 1) uniformly and the mould was placed at room temperature for 24 hours. After that, the cured epoxy composite plate was removed from the mould and the required specimens were cut.

2.5 *Mechanical tests*

After fabrication, the test specimens were subjected to various mechanical tests as per ASTM standards. The standards followed were ASTM- D 638 and ASTM-D 256 for tensile and impact tests, respectively. The tensile tests were conducted at a speed of 2 mm/min at room temperature (303 K). Izod impact tests were conducted for all specimens at room temperature to evaluate the resistance of the material to fracture.

3. Results and Discussion

3.1. *Characterization of Te NWs*

The formation of Te NWs was confirmed by optical and microscopic studies. Fig. 2A shows the absorption spectrum of Te NWs after removing the excess surfactant, impurities and again redispersion in distilled water. Absorption spectrum shows two characteristic Te NW peaks in the range of 250 to 900 nm. According to the Hartree–Fock– Slater study, peak I located in the range of 280-300 nm (4.1–4.4 eV) is due to the transition from the valence band (p-bonding VB2) to the conduction band (p-antibonding CB1), and peak II located in the range of 650-750 nm (1.6–1.9 eV) is assigned to be the transition from the valence band (p-lone-pair VB3) to the conduction band (p-antibonding CB1). Peak II is characteristic peak of length of the NW. Increasing the length of Te NWs will shift the peak II to a higher wavelength region. In our case, peak I was centered at 293 nm and peak II was centered at 720 nm.

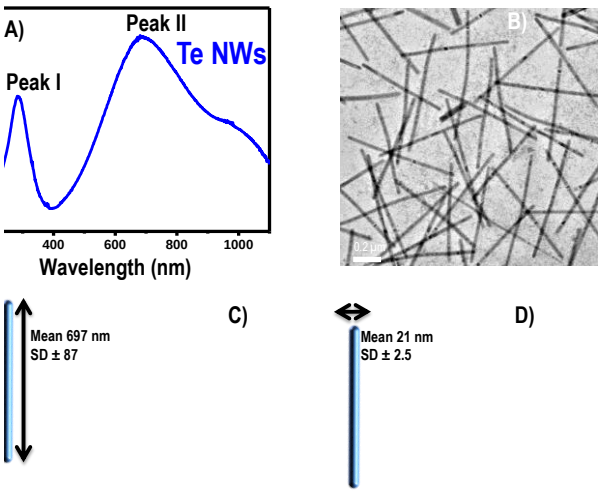

Fig. 2. A) UV/vis spectrum of Te NWs. B) Large-area TEM micrograph of the Te NWs shows without any bending in their morphology. C) and D) are histograms representing the length and diameter distribution of the Te NWs before adding to epoxy system.

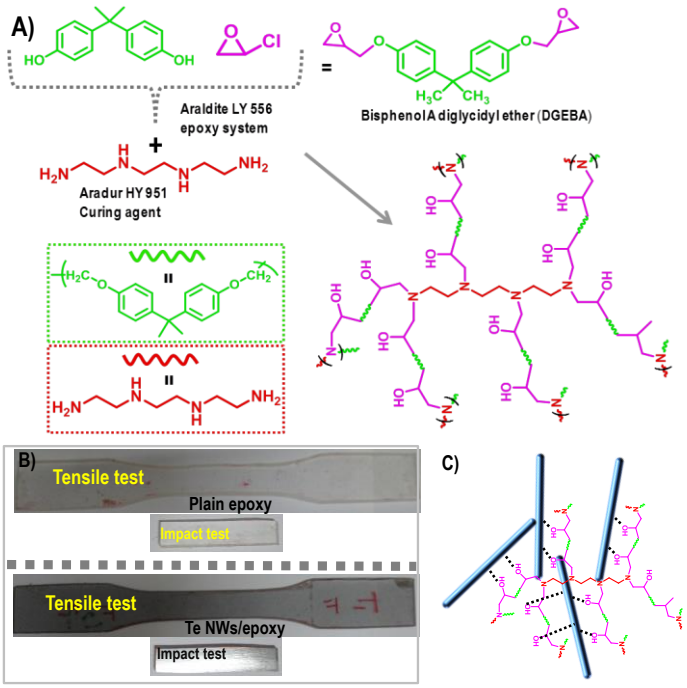

Fig. 3. A) Schematic representation of epoxy polymerization. B) Photographs of one set of specimens of plain epoxy and Te NWs/epoxy used for tensile and impact tests. Note that Te NWs/epoxy specimens are uniformly transparent with pale blue color of Te NWs. This indicates chemisorption of epoxy through –OH groups on active Te NWs surface as represented in scheme C.

From the previous reports,[31,32] the peak I and II positions around 290 nm and 720 nm reveals that the length and width of Te NW were around 690 nm and 20 nm. This sample was analyzed with TEM to find the exact length and width of the Te NWs. The sizes of the Te NWs were in agreement with the length obtained from the absorption spectrum. Fig. 2B shows the large-area TEM image of Te NWs. It shows the Te NWs wires are monodispersed, straight, pretty clean and free from extra surfactant (SDS). Te NWs were structurally uniform and there were no defects, indicating that the Te NWs are single crystals. Fig.2C&D show the length and width histogram of the Te NWs distributions, respectively. Length of NWs is 697±87 nm and diameter of NWs is 21±2.5 nm. From the literature, it is known that three representative planes of t-Te NWs, with interplanar spacings of 0.59, 0.39, and 0.22 nm corresponding to {001}, {010}, and {110}, respectively.[32]

Mechanism of formation of epoxy composites are given in Fig. 3A. Photographs of the plain and Te NWs/epoxy nanocomposites were compared in Fig. 3B. Dog bone shaped specimens were used for tensile tests and rectangular used for the impact test. Even at 0.05 Wt.% of Te NWs, the Te NWs/epoxy specimens are uniformly transparent with pale blue color showing the uniform mixing of Te NWs with epoxy resin. The possible interactions between epoxy and Te NWs surface were represented in Fig. 3C. These interactions are expected to be chemisorption of epoxy –OH groups on active Te NWs surface.

We have performed wide-angle XRD and DSC thermal analysis methods on these samples. Fig. 4A shows the XRD pattern of plain epoxy powder and the Te NWs based epoxy nanocomposites, respectively. As illustrated in Fig. 4A, the cured networks of plain and Te NWs/epoxy samples are amorphous in nature due to the highly cross-linked structures. For the pure epoxy samples, a broad peak centered at 2θ = 18.5˚ is observed which is assigned to the amorphous structure of the epoxy. After addition of Te NWs into the epoxy matrix, this peak shifted towards to lower values and reach to 2θ = 17.3˚. The downward shifting of this peak in the Te NWs/epoxy composites clearly shows that the embedding of Te NWs into epoxy resin influences the microstructure of the composites by the means of interfacial interaction between the Te NWs and epoxy matrix. Importantly, the peak at 2θ = 17.3 in Te NWs/ epoxy sample was sharp in comparison to plain epoxy sample. The full width at half maximum (FWHM) for plain epoxy and Te NWs/epoxy are around ≈10 and ≈ 6 respectively. This indicates the increase in the crystallinity of epoxy structure upon the Te NWs insertion.

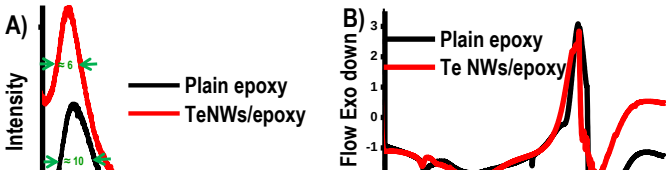

Fig. 4. A) Comparison of the XRD patterns of plain epoxy and Te NWs/epoxy specimens. B) DSC-thermograms of plain epoxy and Te NWs/epoxy specimens.

Fig. 4B shows the DSC-thermograms obtained by thermal decomposition of plain and Te NWs/epoxy specimens. Both samples show two peaks, one is endothermic and another is exothermic peak. The exothermic peaks at low temperature (78 ^{o}C for plain epoxy and 75 ^{o}C for Te NWs epoxy) are corresponding to their melting points. The endothermic peak around 350 ^{o}C corresponding to the thermal decomposition of epoxy polymer. However, tellurium usually shows the sharp exothermic transition around 420^{o}C is absent. The lack of this peak is due to presence of low content of Te NWs. DSC analysis confirms that the amount of Te NW used in epoxy is at very low amount.

3.2. Mechanical Properties

The impact strength and tensile strength values of the plain and Te NWs/epoxy composites are tabulated in Table 1&2. The mechanical properties reported here show that, Te NWs/epoxy specimens are significantly stronger than the plain epoxy specimens.

3.2.1. *Impact properties*

We have conducted Izod impact test on epoxy and Te NWs/epoxy composites as per ASTM D 256 standard. The specimens of 13 mm (width) ×3 mm (thick) × 65 mm (length) were tested. The impact property of the material is its capacity to absorb and dissipate energies under impact or shock loading. The impact energy obtained from un-notched

specimens of epoxy and Te NWs/epoxy was studied by pendulum type Izod impact testing machine of Karl Frank Gmbh 53568 as per ISO180-1982. It is observed that the impact strength tremendously increased on Te NWs/epoxy composite than plain epoxy matrix. The impact resistance values are shown in Table 1. Significant increase in impact strength was observed by incorporation of low amount of filler such as 0.05 % by weight of Te NWs. The plain epoxy had very low impact resistance. Te NWs/epoxy composite material showed impact of 0.4 J/mm, which was almost twice the value of pure epoxy resin, 0.2 J/mm. The impact strength increased by 100 % with the low content of Te NWs. It was about 2 times than that of the plain epoxy. From this study, it was observed that even at low amounts of Te NWs, epoxy nanocomposites exhibit improved mechanical properties. The experimental results show that the presence of Te NWs helps to arrest crack-propagation and efficient stress transfer between epoxy polymer and Te NWs, which results in increased strength.

Specimen	Energy Observed (J)	Impact Strength (J/mm)
Te NW/Epoxy	1.2	0.4
Plain Epoxy	0.7	0.2

Composite	Load at Break(N)	Extension at Break (mm)	Max. Tensile Strength (MPa)	% Elongation	Modulus (Automatic) (Mpa)
Te NWs/Epoxy	1394.1	3.889	31.1	6.2	751.7
Plain Epoxy	1480.2	2.41	28.1	4.0	804.1

Table 1& 2: Impact (top) and Tensile (bottom) test results of plain epoxy and Te NWs/epoxy composite, respectively.

3.3.2. *Tensile properties*

Fig. 5. Tensile properties of plain epoxy and Te NWs/epoxy specimens.

The tensile strength of the nanocomposites depends on the filler-matrix interaction. The dog bone specimens with gauge length 50 mm were cut from the plate as per ASTM D638 standard and tested using Instron Universal testing machine with cross head speed of 2 mm/min. The results are shown in Table 2. The neat resin without any reinforcement had 28.1 MPa tensile strength and modulus of 804.18 MPa. Incorporation of 0.05 % by weight of Te NWs material resulted in 31.1 MPa tensile strength and modulus of 751.69 MPa. Te NWs/epoxy tensile strength was nearly 10.6 % improved. Extension at break, % Elongation also increased which means that ability to absorb energy and ductility of epoxy has been increased due to the presence of Te NWs. From the Fig. 5, it is can be clearly seen that the area under curve has been increased greatly for epoxy-Te NWs nanocomposites, representing increased ability to absorb the energy, which is one of the most desirable properties of epoxy composites for aerospace and automobile structural applications.

3.3. SEM Characterization

In order to understand the interfacial adhesion between Te NWs and epoxy matrix fractured surface, plain and Te NWs/epoxy were further analyzed with SEM imaging and data were shown in Fig. 6, 7 and 8. Fractured surface of the pure epoxy was imaged at different magnifications to see the surface property (Fig. 6). However, we haven't observed any noticeable differences in surface smoothness of plain and Te NWs/epoxy composites as shown in Fig. 6 and 7.

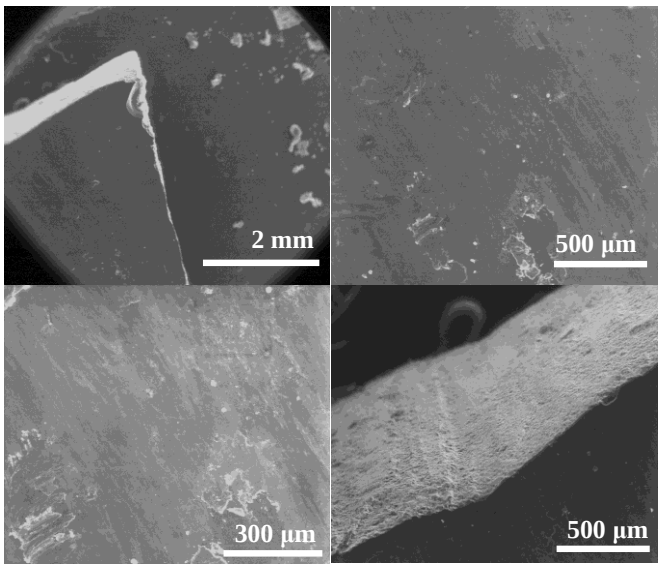

Fig. 6. SEM images of plain epoxy collected at different magnifications (2 mm, 500 µm and 300 µm).

Instead, in comparison to plain, the Te NWs incorporated epoxy composites showed additional features (long chain-like networks) on their surface. Initially, it is expected that they might be scratches, but upon close observation they look different from the regular scratches. Regular scratches appear very continuous (without any breaks) and appear like bright shiny lines and without any structure. These lines are due to the noise resulting from the charging effect, which are commonly observed in the SEM analysis of non-conductive samples. These lines were marked with red dotted boxes in Fig. 7D. Another kind of structures was observed and they are the chain-like arrangement of Te NWs. From the close

observation these chain like structures they are quite different from the noise. These structures are composed of nanoislands (50 to 200 nm) of Te NWs belts. These structures are marked with black arrows in Fig. 7D.

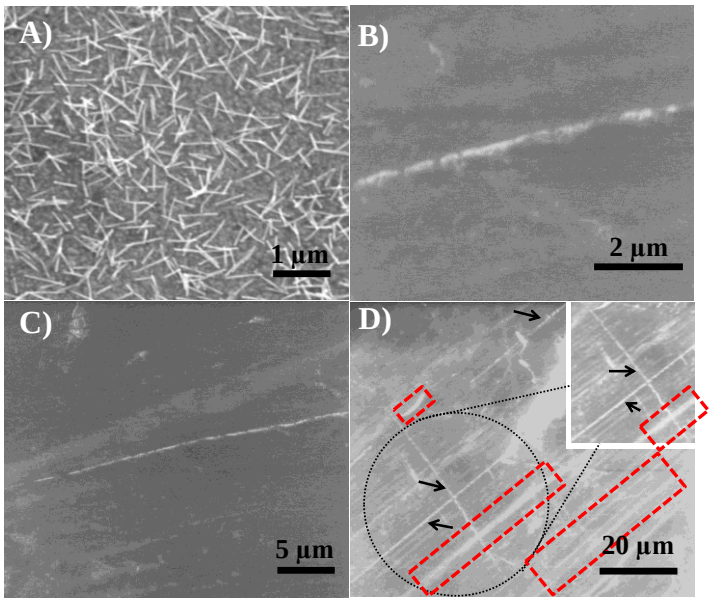

Fig. 7. A) SEM image of Te NWs. Images B, C and D are the SEM image of Te NWs/epoxy composites showing the presence of linear self-assembly of Te NWs into chains. In image D) two kinds of marks are given to show the difference between the self-assembled Te NWs and scratches. Black arrows indicating the self-assembly of Te NWs, red dotted boxes indicating the noise. Inset of D is the enlarged portion of black dotted circle of image D.

This kind of Te NWs belt arrangement was observed throughout the fractured surface of Te NWs/epoxy. No obvious pull out was be observed. The epoxy matrix appears, it was sufficiently wet with the Te NWs. The Te NWs belts were evenly spanned long distances of up to several hundred micrometers. For example, Fig. 8 showed the Te NW belts of 100 µm length.

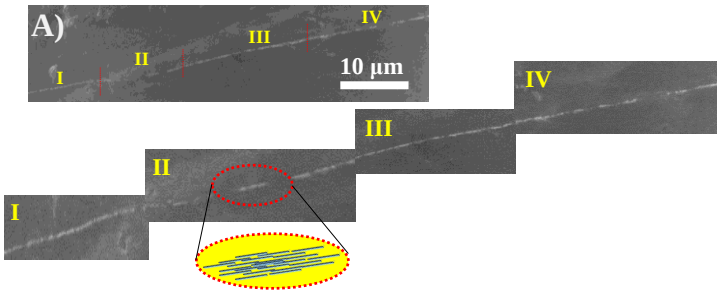

Fig. 8. A) SEM image of Te NWs chain in Te NWs/epoxy composite with length around 100 µm. In order to confirm the presence of Te NWs, we collected the same image at four different magnifications. They are labeled as I, II, III and IV. From all parts, it is clear that the NWs are continuous with some gaps. It is more obvious in part II. One such gap is shown with red dotted circle (part II) and schematically represented the possible arrangement of Te NWs.

As can be seen from the magnified portion of Fig. 8 (I, II, III, and IV) these belts are broken in some places but follow the linear patterns with some bending. These kinds of belts were governed by the chemical interaction between epoxy and Te NWs. This can suggest a regular distribution and dispersion of Te NW within epoxy matrix as shown in the scheme of Fig. 8II. The incorporation of Te NWs in epoxy matrix resembles the insertion of iron rods in concrete, which help to improve the mechanical properties. The fracture surface of Te NW/epoxy composites is rough due to those Te NW belts, this further suggests that the strong interfacial adhesion between Te NWs and epoxy matrix and present strong filler-matrix interfacial bonding and encourages dispersion. However, the belts formation of Te NWs has to confirm by back scattered SEM (which is more sensitive to differences in atomic mass) or some other material sensitive techniques such as TEM with a microtomed sample.

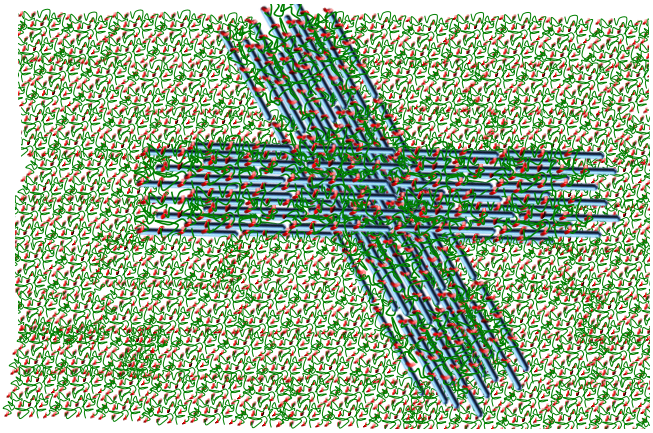

Fig. 9. Schematic representation of arrangement of self-assembly of Te NWs to linear chains in epoxy matrix. Red groups are hydroxyl groups which helps to direct the Te NWs (represented with blue color rods) into Te NW chains. Green portion is polymer backbone.

From the microstructure examination of Te NWs/epoxy nanocomposites by SEM showed the possibility of side by side and end to end self-assembly of Te NWs into linear structures inside the epoxy composite. The reasons behind the improved mechanical properties of Te NWs/epoxy composites are attributed to 1) stronger interaction between the Te NWs and epoxy, and 2) the self-assembly of a group of stacked Te NWs into linear fashion, also called unity effect. The effect can be visualized similar to the iron rods in concrete as shown in Fig. 9.

4. Conclusions

This study provided the reinforcing influences of Te NWs on epoxy resin composites. Even at low wt% (0.05%) of Te NWs in epoxy nanocomposites show remarkable enhancement in the mechanical (impact and tensile) strength. Mechanical properties of Te NWs/epoxy nanocomposite show that Te NWs are good fillers to enhance the strength of the epoxy polymer. SEM results showed that these Te NWs were self-assembled linearly through side by side and end to end fashion. These results could provide guidelines to the

future design of nanocomposites by taking the advantage of Te NWs.

Acknowledgements:

The authors gratefully acknowledge the help and support rendered by the staff members namely Mr. Roch and Ms. Vasanthi of Indian Institute of Technology, Madras for helping out in the testing of materials. Dr. A. George (Hindustan University) for his valuable discussions.

References:

[1] M. A. Rafiee, J. Rafiee, Z. Wang, H. Song, H., Z. Yu, and N. Koratkar. "Enhanced mechanical properties of nanocomposites at low graphene content," ACS nano, Vol. 3, no. 12, 3884-3890, 2009.

[2] K. Naito, "Tensile Properties of Polyimide Composites Incorporating Carbon Nanotubes-Grafted and Polyimide-Coated Carbon Fibers," J. Mater. Eng. Perform., vol. 23,no. 3245, pp 3245-3256, 2014.

[3] N. Kavitha, M. Balasubramanian, and A. Xavier Kennedy. "Investigation of impact behavior of epoxy reinforced with nanometer-and micrometer-sized silicon carbide particles," J. Comp. Mater., 0021998312451920, 2012.

[4] T. P. Mohan, M. R. Kumar, and R. Velmurugan, "Mechanical and barrier properties of epoxy polymer filled with nanolayered silicate clay particles," J. Mater. Sci., vol. 41, no. 10 pp. 2929–2937, 2006.

[5] S. H. Aboubakr and U. F. Kandil, and M. R. Taha. "Creep of epoxy–clay nanocomposites adhesive at the FRP interface: A multi-scale investigation," Int. J. Adhes. Adhes. vol. 54, pp. 1–12, 2014.

[6] D. Galpaya, M. Wang, M. Liu, N. Motta, E. Waclawik, and C. Yan,"Recent Advances in Fabrication and Characterization of Graphene-Polymer Nanocomposites," Graphene, vol. 1, pp.30-49, 2012.

[7] S. Shivakumara and T. R. Penki, and N. Munichandraiah. "Preparation and electrochemical performance of porous hematite (α-Fe_2O_3) nanostructures as super capacitor electrode material," J. Solid State Electrochem., vol. 18, pp.1057–1066, 2013.

[8] J. Zhu, S. Wei, J. Ryu, L. Sun, Z. Luo, and Z. Guo, Magnetic epoxy resin nanocomposites reinforced with core−shell structured Fe@FeO nanoparticles: fabrication and property analysis. ACS Appl. Mater. & Interfaces, vol. 2, no. 7, pp. 2100-2107, 2010.

[9] P. Yanlin, S. Deng, P. Lakshminarayana, G. Nengyue, Y. Peiyan, C. H. Sow, and Q. H. Xu. "Plasmon-enhanced photocatalytic properties of Cu_2O nanowire–Au nanoparticle assemblies," Langmuir, vol. 28, no. 33 pp. 12304-12310, 2012.

[10] T. Udayabhaskararao, and T. Pradeep. "Luminescent Ag_7 and Ag_8 Clusters by Interfacial Synthesis," Angew. Chem. Int. Ed., Vol. 49, pp. 3925-3929, 2010.

[11] P. K. Jain, K. S. Lee, I. H. El-Sayed, and M. A. El-Sayed. "Calculated absorption and scattering properties of gold nanoparticles of different size, shape, and composition: applications in biological imaging and biomedicine," J. Phys. Chem. B, vol. 110 no. 14, pp.7238-7248, 2006.

[12] Y. Gao, S. Wang, H. Luo, L. Dai, C. Cao, Y. Liu, Z. Chen and M. Kanehira,"Enhanced chemical stability of VO_2 nanoparticles by the formation of SiO_2/VO_2 core/shell structures and the application to transparent and flexible VO_2-based composite foils with excellent thermochromic properties for solar heat control," Energy Environ. Sci., vol. 5, pp.6104-6110, 2012.

[13] S. A. B. Hasan, M. M. Dimitrijevic, S. A. Ben hasani, M. M. Dimitrjevic, A. Kojovici, D. B. Stojanovic, K. Obradovicduricic, R. M. J. Heinemanni and R. Aleksic, "The effect of the size and shape of alumina nanofillers on the mechanical behavior of PMMA matrix composites," J. Serb. Chem. Soc. vol. 79, no. 10, pp. 1295–1307, 2014.

[14] P. K. Nayak, and T. R. Penki, "High Li storage capacity of poorly crystalline porous δ-MnO_2 prepared by hydrothermal route," J. of Electroanal. Chem. vol. 703, pp. 126–134, 2013.

[15] S. Stankovich, D. A. Dikin, G. H. B. Dommett, K. M. Kohlhaas, E. J. Zimney, E. A. Stach, R. D. Piner, S. T. Nguyen and R. S. Ruoff, "Graphene-Based Materials," Nature, vol. 442, pp.282-286. 2006.

[16] J. N. Coleman, U. Khan, W. J. Blau, and Y. K. Gunko, "Small but strong: A review of the mechanical properties of carbon nanotube-polymer composites," Carbon, vol. 44, no. 9, pp.1624 – 1652, 2006.

[17] S. Y. Yang, W. N. Lin, Y. L. Huang, H. W. Tien, J. Y. Wang, C. C. M. Ma, S. M. Li, and Y. S. Wang."Synergetic effects of graphene platelets and carbon nanotubes on the mechanical and thermal properties of epoxy composites," Carbon, vol. 49, no. 3, pp.793-803. 2011.

[18] R. V. Kurahatti, and A. O. Surendranathan."Defence applications of polymer nanocomposites," Def. Sci. J, vol. 60, no. 5, pp. 551-563, 2010.

[19] J. Njuguna, and K. Pielichowski. "Polymer nanocomposites for aerospace applications: properties," Adv. Eng. Mater, Vol. 5,No. 11, pp.769-778, 2003.

[20] F. Gao. 2012, "Advances in Polymer Nanocomposites - Types and Applications," Woodhead Publishing Ltd., UK, chap. 15.

[21] W. K. Hendricks. "The Epoxy Book", System Three Resins, Inc., 2000.

[22] K. Pashayi, and H. R. Fard, F. Lai, S. Iruvanti, J. Plawsky and T. Borca-Tasciuc." High thermal conductivity epoxy-silver composites based on self-constructed nanostructured metallic networks," J. Adv. Mater. Vol. 111, pp. 104310-104316, 2012.

[23] N. H. MohdHirmizi, M. Abu Bakar, W. L. Tan, N. H. H. Abu Bakar, J. Ismail, and C. H. See. "Electrical and Thermal Behavior of Copper-Epoxy Nanocomposites Prepared via Aqueous to Organic Phase Transfer Technique," J. Nano. Mat., Article ID 219073, 11 pages, 2012.

[24] H. Gu, S. Tadakamalla, Y. Huang, H. A. Colorado, Z. Luo, N. Haldolaarachchige, D. P. Young, S. Wei, and Z. Guo "Polyaniline Stabilized Magnetite Nanoparticle Reinforced Epoxy Nanocomposites," ACS Appl. Mater. Interfaces, vol. 4,, no. 10 pp.5613−5624, 2012.

[25] A. Chatterjee and M. S. Islam. "Fabrication and Characterization of TiO_2 Epoxy Nanocomposite," Mater. Sci. Eng., vol. 487, no. 1-2 pp.574–585, 2008.

[26] Y. Wu, L. Song and Y. Hu. "Fabrication and Characterization of TiO_2 Nanotube Epoxy Nanocomposites," Ind. Eng. Chem. Res., vol. 50, no. 21, pp. 11988–11995, 2011.

[27] B. Reddy. "Advances in Nanocomposites - Synthesis, Characterization and Industrial Applications," In Tech, US, chap. 32, 2011.

[28] Z. Wang, H. Zhao, L. Fan, J. Lin, P. Zhuang, W. Z. Yuan, Q. Hu, J. Z. Sun, B. Z. Tang "Chitosan rods reinforced by aligned multiwalled carbon nanotubes via magnetic-field-assistant *in-situ* precipitation," Carbohydrate Polym, vol. 84, no. 3, pp.1126-1132, 2011.

[29] P. Tangney and S. Fahy. "Density-functional theory approach to ultrafast laser excitation of semiconductors: Application to the A1 phonon in tellurium" Phys. Rev. B, vol. 65, pp.054302-13, 2002.

[30] S. Dey and V. K. Jain, "Platinum Group Metal Chalcogenides: Their Syntheses And Applications In Catalysis And Materials Science," Platinum Metals Rev., vol. 48, no. 1, pp.16-29, 2004.

[31] Z. H. Lin, Z. Yang and H. T. Chan. "Preparation of Fluorescent Tellurium Nanowires at Room temperature," *Cryst. Growth Des.*, vol. 8, no. 1, pp 351–357, 2008.

[32] T. S. Sreeprasad, A. K. Samal, and T. Pradeep."Bending and Shell Formation of Tellurium Nanowires Induced by Thiols," Chem. Mater., vol. 21, No. 19, pp 4527–4540, 2009.

[33] B. Mayers, and Y. Xia. "Formation of Tellurium Nanotubes through Concentration Depletion at the Surfaces of Seeds," Adv. Mater., vol. 14, no. 4, pp.279-282, 2002.

[34] M. Mo, J. Zeng, X. Liu, W. Yu, S. Zhang, and Y. Quin. "Controlled Hydrothermal Synthesis of Thin Single-Crystal Tellurium Nanobelts and Nanotubes," Adv. Mater., vol. 14. no. 22, pp. 1658-1662, 2002.

[35] Y. J. Zhu, W. W. Wang, R. J. Qi and X. L. Hu." Microwave-assisted synthesis of single-crystalline tellurium nanorods and nanowires in ionic liquids," Angew. Chem., vol. 116, no. 11,pp 1434-1438, 2004.

[36] Q.Y. Lu, F. Gao, and S. Komarneni, "Biomolecule-Assisted Reduction in the Synthesis of Single-Crystalline Tellurium Nanowires," Adv. Mater., vol. 16, no. 18, pp.1629–1632, 2004.

[37] B. Geng, Y. Lin, X. Peng, X, G. Meng, and L. Zhang." Large-scale synthesis of single-crystalline Te nanobelts by a low-temperature chemical vapour deposition route," Nanotech., vol. 14, no. 9, pp. 983–986, 2003.